Electronic Supplementary Material (ESI) for Physical Chemistry Chemical Physics.
This journal is © the Owner Societies 2018

Single-molecule fluorescence enhancement of a near-infrared dye by gold nanorods using DNA transient binding

Supplementary Information

Weichun Zhang, Martín Caldarola, Xuxing Lu, Biswajit Pradhan, Michel Orrit
Huygens-Kamerlingh Onnes Laboratory, Leiden University, 2300 RA Leiden, Netherlands
orrit@physics.leidenuniv.nl

Contents

1 Sample preparation

Materials. Methanol (99.8%), (3-Mercaptopropyl)trimethoxysilane (MPTS, 95%), cysteamine (98%), 4-(2-Hydroxyethyl) piperazine-1-ethanesulfonic acid (HEPES, 99.5%), bovine serum albumin (BSA, 96%), tris(2-carboxyethyl) phosphine hydrochloride (TCEP, 98%) were purchased from Sigma-Aldrich; Sodium acetate (CH3COONa, 99%) from Merck; NeutrAvidin (NA) protein and succinimidyl 4-(p-maleimidophenyl)butyrate (SMPB) from ThermoFisher. HEPES buffer (10 mM) was prepared by dissolving HEPES in milli-Q water and the pH was adjusted to 7. Acetate buffer (pH 4) was prepared from acetic acid and sodium acetate. All the DNA oligonucleotides including the single strand DNA labeled with IRDye800CW (imager-IRDye800CW) were purchased from Integrated DNA Technologies, Inc. The sequence of imager-IRDye800CW is 3'-TAT GTA GAT C-5'-IRDye800CW. Gold nanorods were purchased from Nanopartz Inc. (A12-40-780-CTAB). The average size is 38 nm $\times$ 118 nm by diameter and length.

Silanization of the coverslip surface. Glass coverslips (Menzel-Gläser, ϕ = 25 mm, No. 1) were cleaned and silanized before further functionalization. The coverslips were sonicated in water (20 min) and ethanol (20 min). They were dried with a clean nitrogen flow and then immersed for 30 minutes with gentle stirring in a methanol solution containing 1% (3-mercaptopropyl)trimethoxysilane (Sigma-Aldrich) and 5% glacial acetic acid in a Teflon incubator. Thereafter, the silanized slides were washed thoroughly with methanol and dried with a nitrogen flow. This results in binding of the silane groups to the active hydroxyl groups and creates a thiol surface that can be used for conjugation with gold nanorods and for passivation of the substrate surface. If not immediately used for the next step, they were stored inside a desiccator to maintain the activity of the thiol groups.

Gold nanorod immobilization. The suspension of gold nanorods we purchased is stabilized with cetyl trimethyl ammoniumbromide (CTAB). In order to immobilize the nanorods on a thiolated glass surface, we decreased the concentration of CTAB by centrifugation and resuspension in milliQ water. This solution of nanorods was in contact with the thiol-activated glass coverslip for 30 minutes. Unbound gold nanorods were washed away with milliQ water. This procedure resulted in around 6 isolated single gold nanorods per 100 μm^2 area immobilized on the substrate.

Docking DNA on gold nanorods. The coverslip with gold nanorods was treated with a mixture of thiolated docking DNA strands, methoxy-poly(ethylene glycol)-thiol (mPEG7-SH, MW = 350), 5 mM NaCl and 1 mM Tris(2-carboxyethyl)phosphine hydrochloride (TCEP) in 0.1 M acetate buffer at pH = 4. The sequence of the docking strand was DTPA-5'-ATA CAT CTA GAA ATT-3'. DTPA represents dithiol phosphoramidite, which strongly binds the docking strands to the gold nanorods. The average number of docking strands on a gold nanorod can be controlled by the concentration ratio between docking strands and mPEG7-SH, which was kept at around 1:1000 to ensure only a few docking strands sat at the tips of a nanorod. TCEP was used to prevent the formation of disulfide bonds and thus maintain the reactively of thiol groups. The incubation lasted overnight and the coverslip was washed extensively with HEPES buffer.

To prevent non-specific sticking of imager strands to the surface, the rest of the glass surface

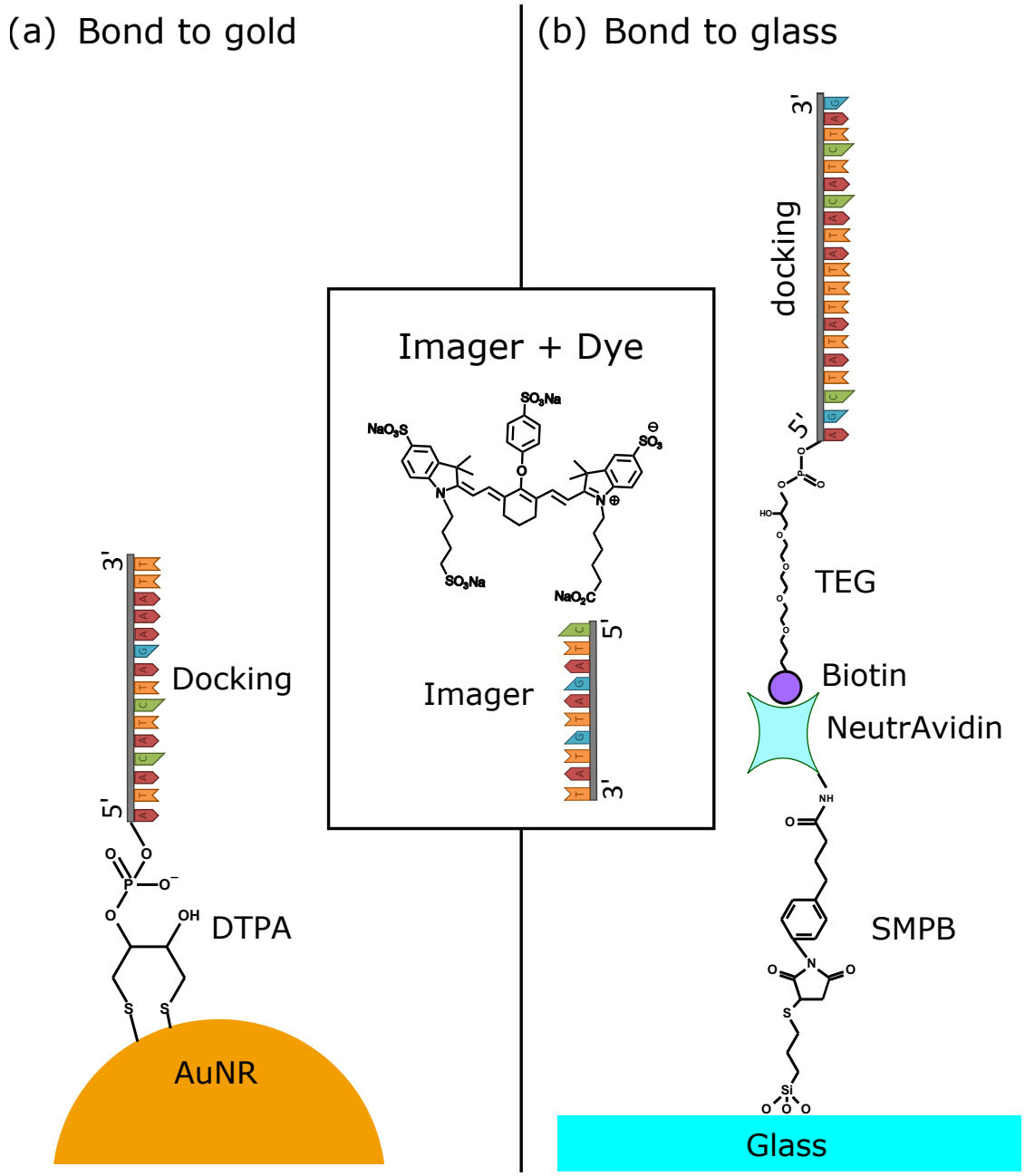

Figure S1: Schematic representation of the bonds used to attach the docking strand to the gold surface (a) and glass surface (b). The inset in the middle shows the imager DNA strand and the dye structure, which is the same for both cases.

was passivated with bovine serumalbumin (BSA). This was achieved by incubating the coverslips with 1 mM succinimidyl 4-(p-maleimidophenyl)butyrate (SMPB), 20 μM BSA and 1 mM TCEP in HEPES buffer for 2 hours. SMPB is a cross-linker that contains an amine-reactive end (N-hydroxysuccinimide ester) and a thiol-reactive end (maleimide), thereby binding BSA to the substrate. The unreacted chemicals were removed by washing with HEPES buffer. The functionalized coverslip was used immediately or stored in HEPES buffer.

The chemical structure used for this situation is shown in Figure S1(a).

Docking DNA on glass substrate. The coverslip with gold nanorods was treated with 100 μM cysteamine and TCEP in 0.1 M acetate buffer at pH = 4 for at least 2 hours to passivate the surface of nanorods. After the slide was washed with HEPES buffer, it was treated with a solution with 1 μM NeutrAvidin (NA), 10 μM SMPB and 1 mM TCEP in HEPES buffer (pH = 7). SMPB is a cross-linker that immobilizes NA protein molecules onto the glass substrate. The incubation lasted 90 min and excess reagents were washed away by HEPES buffer. Lastly, 100 nM docking DNA strand in HEPES buffer was applied to the coverslip. The sequence of the docking strand was biotinTEG-5'-A GCT ATA TTT ATA CAT CTA G-3'. Biotin-TEG increases the oligo-biotin distance to 15 atoms using a triethyleneglycol (TEG) spacer. The biotinylated oligonucleotides binds strongly to the NeutrAvidin molecules. After 30 minutes, the coverslip was washed with HEPES buffer. The functionalized coverslip was used immediately or stored in HEPES buffer.

The chemical structure used for this situation is shown in Figure S1(b).

2 Correction of gold nanorod spectra

The photoluminescence emission of gold nanorods is in the near-infrared range, where the collection efficiency of the optical setup is poor. Therefore, the measured raw spectra have to be normalized by the spectral response of the setup. To this end, we used a standard fluorophore for the near-infrared range, 4-dimethylamino-4'-nitrostilbene (4,4'-DMANS, Sigma-Aldrich), excited with the 532-nm laser. The wavelength-dependent relative detection efficiency was obtained by normalizing the measured fluorescence spectrum by the real emission spectrum of the standard dye [1]. Figure S2 shows the relative response of the setup as a function of wavelength. The measured spectra of nanorods, with the background spectra subtracted, were corrected for the spectral response function and further fitted with a Lorentzian profile to obtain the localized surface plasmon resonance wavelength.

3 Size of the confocal volume

We measured the size of the confocal volume by imaging gold nanorods, which are smaller than the diffraction-limited point-spread function (PSF) of the instrument. We scanned three-dimensional photoluminescence images of a gold nanorod in water excited with the 785-nm laser. As an example, figure S3 shows the yz section of the point spread function (z is along the optical axis). All three sections (xy, xz and yz) of the point spread function were fitted with

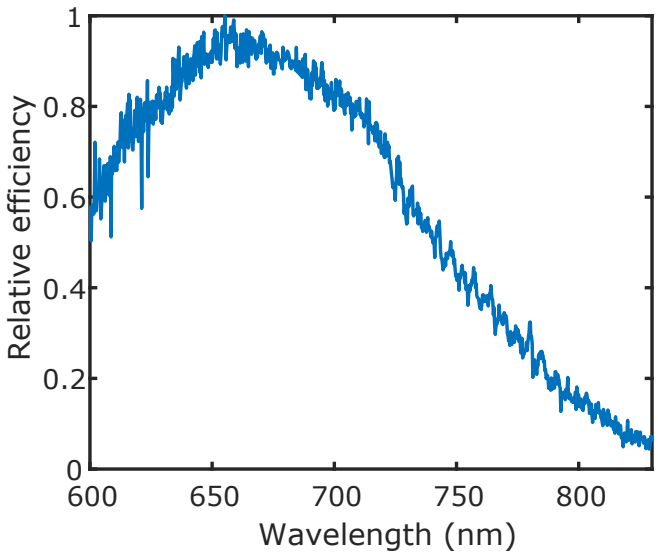

Figure S2: Relative detection efficiency of the setup as a function of wavelength.

two-dimensional Gaussian functions. Taking the xy plane as an example, the model is[2]

$$I = I_0 + I_{\max}\exp\left\{ -2\left[\left(\frac{x-x_0}{w_x}\right)^2 + \left(\frac{y-y_0}{w_y}\right)^2\right]\right\}. \tag{1}$$

(x_0, y_0) is the coordinate of the center of the section and w_x, w_y are the $1/e^2$ radii of the point spread function in the fitting plane. $I_{\max}$ is the maximum photoluminescence intensity and I_0 is the background signal.

Table 1 shows the resulting lateral and axial dimensions from the fitting. The confocal volume is calculated from the mean dimensions in each axis as

$$V_{\text{conf}} = \left(\frac{\pi}{2}\right)^{3/2} w_x w_y w_z = 0.164 \pm 0.002 \text{ fL}. \tag{2}$$

Table 1: Dimensions of the point spread function determined from 2D Gaussian fits

Section	w_x/ nm	w_y / nm	w_z /nm
xy	320 ± 5	276 ± 4	-
xz	327 ± 3	-	873 ± 8
yz	-	300 ± 3	913 ± 8
Mean	324 ± 3	288 ± 3	893 ± 6

4 Saturation of IRDye800CW

We measured the fluorescence intensity from the dye as a function of the excitation power to find the saturation intensity. Figure S4 shows the fluorescence signal from a solution of 100 nM imager-IRDye800CW in HEPES buffer as a function of the excitation power. Fluorescence scales linearly with the excitation power for power lower than 10 μW. With higher power, the curve

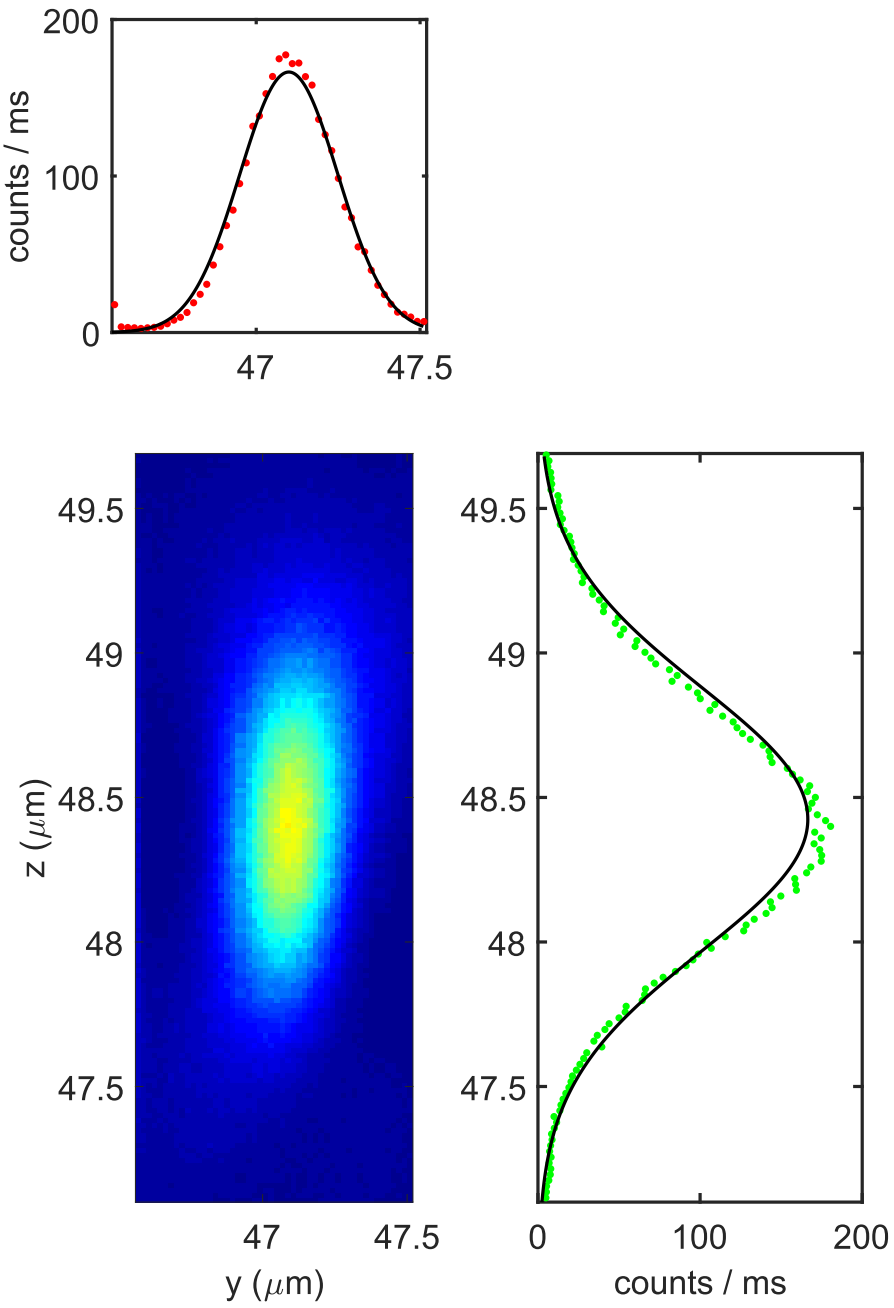

Figure S3: yz section of the point spread function measured with the one-photon luminescence of a gold nanorod. Line profiles through the center are shown. Experimental data are shown as red (along the x axis) and green (along the z axis) dots and the Gaussian fits are represented by black lines.

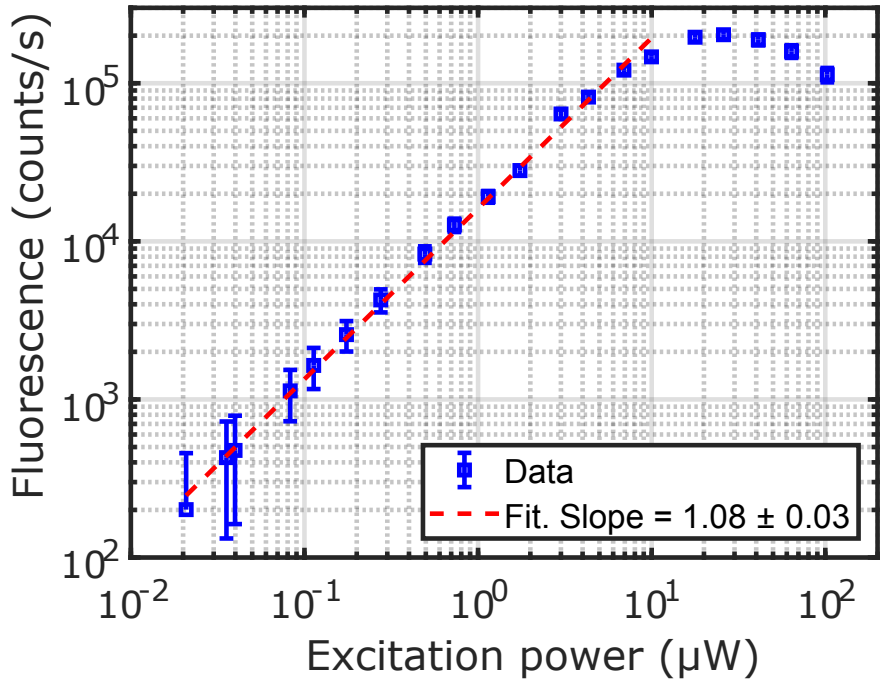

Figure S4: Fluorescence signal from a solution of 100 nM imager-IRDye800CW in HEPES buffer as a function of the excitation power. We found a saturation power of 10 μW.

deviates from the linear relation. The fluorescence intensity decreases with increasing power for excitation power higher than $\sim$ 40 μW, which is attributed to photobleaching. We found a saturation power that is 5000 times higher than the incident power on the gold nanorods for the enhancement experiment. Therefore, we can safely say that the saturation intensity is well above the local field intensity that can be achieved in our enhancement study. Therefore, molecules in the close vicinity of gold nanorods are still well below saturation.

By extrapolating the data and fitting shown in Figure S4, we predict the fluorescence count rate to be 19.7 $\pm$ 3.1 counts/s if excited at 2 nW. For a solution of 100 nM, there are 9.9 $\pm$ 0.1 molecules in the focal volume. These yield a molecular brightness of 2.0 $\pm$ 0.3 counts/s/molecule, used to calculate the enhancement factors.

5 Numerical simulations

The excitation enhancement was calculated with a finite-element method using Comsol Multiphysics. We calculated the near-field intensity map of a single gold nanorod with a size of 38 nm $\times$ 116 nm in water excited at 785 nm. The nanorod is found to be associated with a surface plasmon resonance at 784 nm by calculating extinction cross-sections as functions of wavelength. This size was chosen to ensure the best spectral overlap with the excitation laser and, hence, the largest enhancement factor. The incident plane wave was linearly polarized parallel to the long axis of the nanorod. The dielectric permitivity for gold was taken from Johnson and Christy [4], and the refractive index of the ambient medium was taken as 1.33. The excitation enhancement

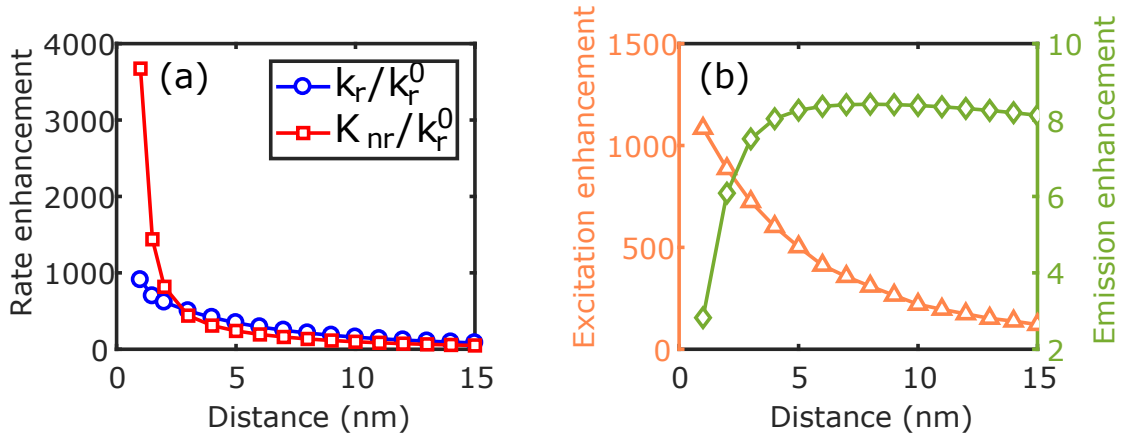

Figure S5: (a) Calculated radiative rate enhancement ($k_\mathrm{r}/k_\mathrm{r}^0$, blue circles) and relative additional nonradiative rate ($K_\mathrm{nr}/k_\mathrm{r}^0$, red squares) of an IRDye800CW molecule as functions of the distance to the tip of the nanorod. (b) Calculated excitation enhancement (orange triangles, left axis) and emission enhancement (green diamonds, right axis) as functions of the distance to the tip of the nanorod.

E_exc is the ratio of local field intensities with and without the nanorod, $E_\mathrm{exc} = |\mathbf{E}|^2/|\mathbf{E}_0|^2$, at the emitter's position.

We used a boundary element method (SCUFF-EM) to evaluate the modifications of decay rates and emission enhancement using a classical electrodynamics approach [5, 6]. An IRDye800CW molecule was modeled as a radiating point dipole oscillating at a frequency which corresponds to an emission wavelength of the molecule. It was assumed that the point dipole is placed along the long axis of the nanorod with a certain distance from the tip and oriented parallel to the revolution axis of the nanorod. All the results were averaged over the actual luminescence spectrum of the molecule. The diameter and length of the nanorod were set as 38 nm and 116 nm respectively. The refractive index of the ambient medium was 1.33, and the dielectric constant for gold was taken from Johnson and Christy [4].

Figure S5 (a) plots the modified radiative (k_r) and nonradiative (K_nr) decay rates relative to the intrinsic radiating rate of the dipole (k_r^0) against the separation between dipole and rod. The competition between k_r and K_nr leads to an emission enhancement that is represented by the green diamonds in Figure. S5 (b). The orange triangles in Figure. S5 show the excitation enhancement, which is calculated by a finite-element method.

6 Calculation of nanorod temperature increase

Because the nanorods are only sparsely scattered on the substrate, bulk heating of the solution can be neglected. Each individual nanorod can be considered as an independent light-induced heat source. The local temperature increase of a nanorod depends upon the absorption cross-section, laser intensity, geometry of the nanorod, and thermal conductivities of the immersion

medium and supporting substrate, as illustrated by the following equation [7]:

$$\Delta T_{\mathrm{NR}} = \frac{\sigma_{\mathrm{abs}} I}{4\pi R_{\mathrm{eq}} \beta \bar{\kappa}}, \tag{3}$$

where σ_{abs} is absorption cross section, I intensity of illumination, R_{eq} the radius of a sphere with the same volume as the nanorod, β a nanorod geometry-dependent coefficient and κ the averaged thermal conductivities of water and glass.

In the calculation, we considered a nanorod with a size of 38 nm $\times$ 116 nm by diameter and length. σ_{abs} at 785 nm was calculated using Comsol Multiphysics to be 5×10^{-14} m^2. $I = 8.8$ kW/cm^2 at the center of the laser focus. For a nanorod, $\beta = 1 + 0.96587\ln^2(\mathrm{AR}) = 2.2$ (AR is the aspect ratio of the nanorod). $\bar{\kappa} = (\kappa_{\mathrm{water}} + \kappa_{\mathrm{glass}})/2 = 1$ W/(m·K). On the basis of these parameters, we calculated a temperature increase of 5.3 K at the surface of the nanorod. Such a local temperature is well below that required for thermally breaking a Au-S bond [8].

7 Flexibility of DNAs

Double-strand DNAs have a persistence length of 50 nm [9]. Therefore a double strand DNA that is a few nm in length can be regarded as straight. So when the imager strand hybridizes with the docking strand, the double-strand part is straight and the length does not change. However, the hybridized DNA may wag because of the flexibility of the tether between the docking strand and the gold or glass surface. Then the position of the fluorophore in the near field may change, resulting in variations in fluorescence intensity because of the strong dependence of fluorescence enhancement on the position of the fluorophore with respect to the tip of the gold nanorod.

In the first experimental approach where the docking DNA strands are attached on the gold surface, the docking DNA strands are surrounded by rigid PEG chains, which are also covalently bound to the gold surface. The fluorescence intensity does not exhibit strong variations when the imager strand hybridizes with the docking strand. To understand this, we tried replacing mPEG7-SH ($\sim$ 3.5 nm in length) with cysteamine, a small molecule with a thiol group ($\sim$ 1 nm in length) and compared their effect on the flexibility of the hybridized strands [10]. Transient-binding traces of a cysteamine-functionalized and of a PEG-functionalized nanorod are presented in Fig. 6. The intensity bursts for the cysteamine-functionalized nanorod are much noisier than the bursts of the PEG-functionalized nanorod. The possible reason is that the steric hindrance by the rigid PEG chains surrounding the docking strand prevents the hybridized DNA from wagging so that the position of the fluorophore does not change with respect to the nanorod.

In the second experimental approach where the docking DNA strands are attached on the glass surface, 1) 10 base pairs on the docking strands remain unhybridized with the imager strand, 2) the tether linking the fluorophore and the glass surface is much longer than in the first approach and 3) the docking DNA strands are not surrounded by PEG chains. Therefore, in this case, the docking strands are more flexible, as the time traces in Fig. 4 in the main text exhibit stronger fluctuations than those in Fig. 2 and Fig. 3 during the high intensity events.

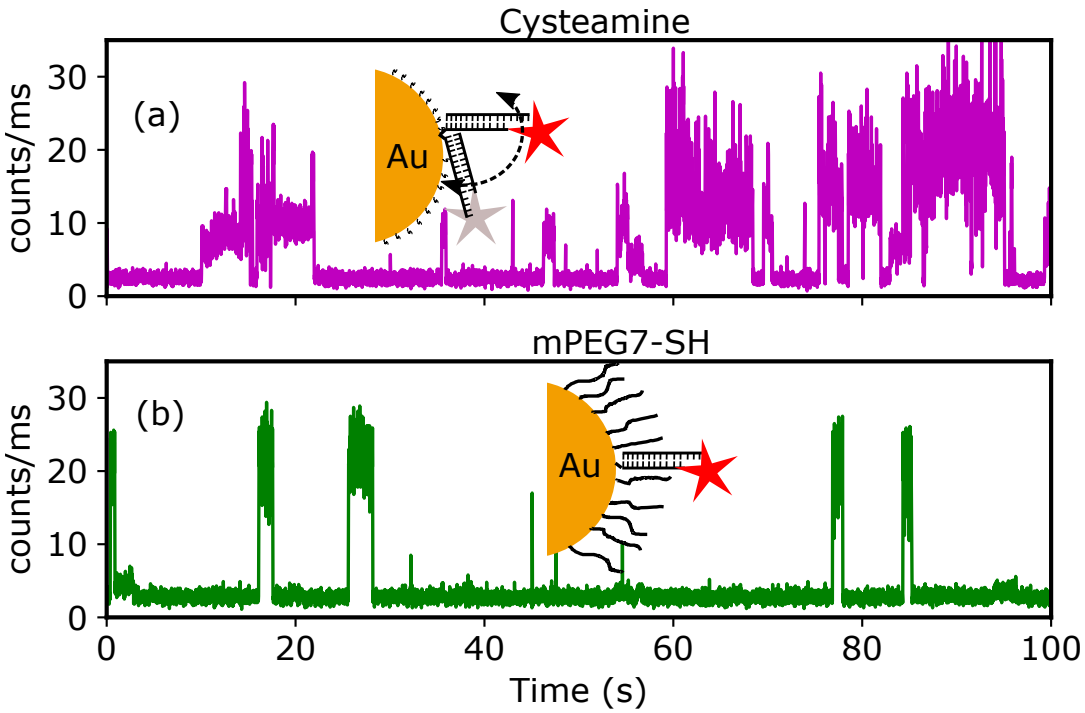

Figure S6: Time traces of transient binding on a gold nanorod using cysteamine (a) and mPEG-SH (b) to control the density of docking strands. The intensity bursts in the case of cysteamine are much noisier while the bursts for the PEGylated nanorod are much more stable.

References

[1] J. R. Lakowicz, Principles of Fluorescence Spectroscopy. Springer US, 3 ed., 2006.

[2] S. Rüttinger, V. Buschmann, B. Krämer, R. Erdmann, R. Macdonald, and F. Koberling, "Comparison and accuracy of methods to determine the confocal volume for quantitative fluorescence correlation spectroscopy," Journal of Microscopy, vol. 232, no. 2, pp. 343–352, 2008.

[3] S. Khatua, P. M. R. Paulo, H. Yuan, A. Gupta, P. Zijlstra, and M. Orrit, "Resonant plasmonic enhancement of single-molecule fluorescence by individual gold nanorods," ACS Nano, vol. 8, no. 5, pp. 4440–4449, 2014.

[4] P. B. Johnson and R.-W. Christy, "Optical constants of the noble metals," Physical Review B, vol. 6, no. 12, p. 4370, 1972.

[5] M. T. Homer Reid and S. G. Johnson, "Efficient Computation of Power, Force, and Torque in BEM Scattering Calculations," ArXiv e-prints, July 2013.

[6] `http://homerreid.com/scuff-EM`.

[7] G. Baffou, R. Quidant, and F. J. García de Abajo, "Nanoscale control of optical heating in complex plasmonic systems," ACS Nano, vol. 4, no. 2, pp. 709–716, 2010.

[8] A. M. Goodman, N. J. Hogan, S. Gottheim, C. Li, S. E. Clare, and N. J. Halas, "Understanding resonant light-triggered DNA release from plasmonic nanoparticles," ACS Nano, vol. 11, no. 1, pp. 171–179, 2016.

[9] G. S. Manning, "The persistence length of DNA is reached from the persistence length of its null isomer through an internal electrostatic stretching force," Biophysical journal, vol. 91, no. 10, pp. 3607–3616, 2006.

[10] B. Pradhan et al., Fluorescence of single copper proteins: dynamic disorder and enhancement by a gold nanorod. PhD thesis, 2018.